Renewable Energy, Environment, and Power Quality Journal (REE&PQJ)
ISSN:3020-531X
Volume 24, January 2026

LCL filter design and experimental response analysis for a SiC inverter

S. Martín-Arroyo[1], A. Llamazares[1], J. Herrero Ciudad[2] and M. García-Gracia[1]

[1] Department of Electrical Engineering
EINA, Zaragoza University
María de Luna 3 – Edificio Torres Quevedo – Campus Río Ebro – 50018 Zaragoza (Spain)

[2] For Optimal Renewable Energy Systems, S.L. Celsa
17 – Polígono PLA-ZA, 50197 Zaragoza (Spain)

Abstract. In this paper, an LCL filter for a 20-kW SiC power inverter with a 25 kHz switching frequency is proposed and assessed. The transfer function without neglecting the network effect is considered. The optimal value of the damping resistor is evaluated to minimize losses while maintaining power quality and device stability. Finally, the harmonic content produced by the SiC inverter is experimentally measured to verify the effectiveness of the LCL filter.

Key words. LCL filter, SiC inverter, harmonic contents, transfer function.

1. Introduction

The renewable energy, wind and photovoltaic solar, have experienced a great boost that will only increase exponentially in the coming years. These sources have a final stage of DC-AC voltage conversion carried out by power inverters using vector modulation techniques, usually PWM, which generate harmonics of the modulation frequency. In this way, the quality of the injected signal can be dangerously disturbed, especially in weak grids and island systems.

The use of devices based on Silicon (Si) has dominated the field of power electronics until recent years. The development of controllable semiconductors such as MOSFET, IGBT or IGCT has allowed power electronic converters to reach high levels of frequency and power. Currently, there is a growing use of wide bandgap (WBG) semiconductor devices, based on SiC and GaN has become widespread. The most commonly used devices are SiC MOSFETs and GaN transistors. WBG semiconductors operate at higher voltages, temperatures, and switching frequencies than Si IGBTs that have been widely used in the recent past. This allows power converters based on SiC or GaN devices to achieve higher efficiency and be smaller and lighter, thus achieving higher power density, with lower heat dissipation requirements. The GaN device is more suitable for low to medium voltage ranges (200 V - 600 V). However, for higher voltage ranges, the SiC device is currently more suitable.

Therefore, the ability of SiC devices to switch at high speed significantly increases power density, both in converters and passive components, reducing their size [1],[2]. The increase in switching speed and frequency in power converters, particularly those based on SiC technology, results in rapid voltage (*du/dt*) and current (*di/dt*) variations, leading to high-frequency EMI. This issue is exacerbated as the switching frequency increases. Currently, typical switching frequencies range from tens to hundreds of kHz, with ongoing research aimed at pushing these frequencies into the MHz range. Consequently, the most significant emissions problems occur across a frequency range from the fundamental switching harmonic to several tens of MHz. EMC standards typically address these issues through conducted emission measures [3]. Given these factors, it will be imperative in the near future to mitigate EMI generated by power converters across a broad frequency spectrum, ranging from several kHz to 100 MHz or more.

In order to meet the requirements for electrical supply quality, the solution used in most systems consists of including an LCL filter at the output of the inverter for grid coupling as shown in Fig. 1. The combination of the inductance and capacitance could create a resonant circuit with the parasitic elements contributing to the overall impedance characteristics. This resonance occurs at a specific frequency determined by the values of L and C, resulting in a peak in the filter's impedance response. Additionally, variations in load conditions or component tolerances can further influence the resonance frequency, leading to potential stability issues if not properly mitigated.

Furthermore, in order to reduce the resonant peak of the LCL filter response and for stability purposes, it is common to adopt a passive damping solution [4]. The optimal configuration of passive damping is achieved by adding a damping resistor in series with the capacitor.

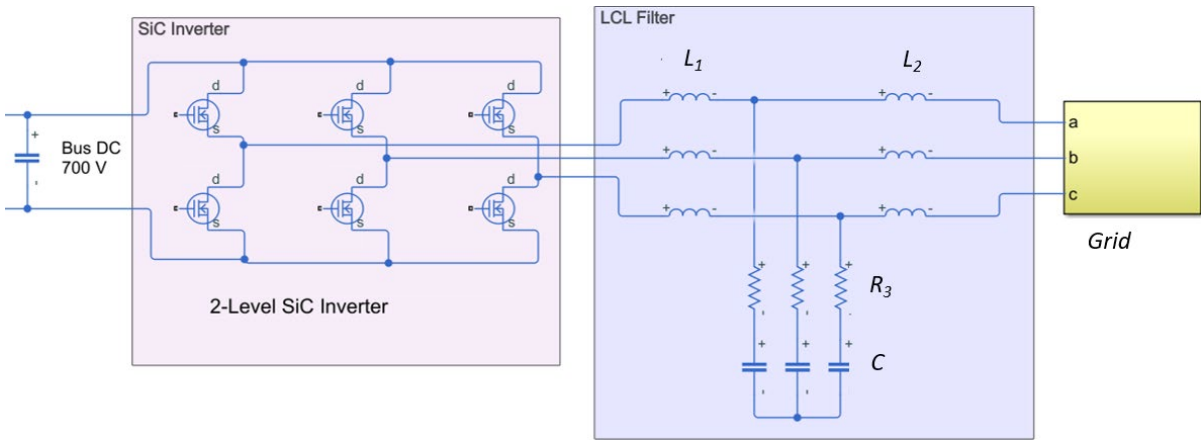

Fig. 1. Grid-connected inverter with an LCL filter.

2. Case study and passive filter topology

In the selection of the filter topology, a balance between size, weight, cost, and power supply quality is sought. L filters act as first-order low-pass filters to attenuate grid-side current harmonics. A first-order filter provides the simplest solution. They are simple, however, a high inductance value is required to achieve the most sinusoidal waveform possible at the converter output, increasing volume, weight, and cost of inverters, as well as causing a greater voltage drop in the inductance and slower system dynamics.

To overcome the disadvantages of first-order filters, power converters generally opt for higher-order passive filters to cancel high-frequency harmonics caused by pulse width modulation (PWM). Even though additional passive components are incorporated, they are generally smaller and lighter than the passive component needed for a first-order filter [5],[6].

An LCL filter is a widely used solution in grid-connected power converters. LCL filters act as third-order low-pass filters, combining an LC filter (second-order low-pass filter) and an L filter (first-order low-pass filter). Although LCL filters are generally smaller and cheaper than L filters, they can cause resonance problems due to the introduction of a capacitor in an inductive environment. Therefore, it is necessary to carefully study the design of the LCL filter to avoid system instabilities.

A. Case study

The considered inverter as a design case study is a 20-kW two-level and three-wire system, as depicted in Fig. 1. It employs sinusoidal pulse-width modulation (SPWM) with a 25-kHz switching frequency (f_{switch}). However, the performance of the filter has also been analysed at higher frequencies, up to 60 kHz.

B. LCL filter transfer function

The LCL filter is designed for a given maximum current ripple, limiting the voltage drop and avoiding possible resonances in the filter. The input parameters considered in the filter design are P (rated active power), f_{switch} (switching frequency), and V_{DC} (DC bus voltage).

However, the main drawback of using an additional damping resistor in the LCL filter is the additional power losses, which requires the sizing of the heat sink (radiator). It can be replaced by a notch-type active filter, although this solution introduces a delay with consequences from the stability point of view.

A very low value of the damping resistor results in unstable operation. On the other hand, when the damping resistor value increases, the effectiveness of the LCL filter is reduced. The passive resistor must be adequate to avoid instabilities but, at the same time, it must not cause losses that can reduce the LCL filter effectiveness. So, a compromise between these two factors has to be reached.

The frequency response of the LCL filter is analysed by its transfer function with and without the damping resistor, as shown in Fig. 2. $G_v(s)$ is the ratio of output current I_2 to input voltage V_1 while output V_2 is short-circuited:

$$G_v(s) = \frac{-I_2}{V_1} = Y_{21} = \frac{-I_2}{V_1}\Big|_{V_2=0} \tag{1}$$

$$G_v(s) = \frac{R_3+\frac{1}{sC}}{s^2+As+\frac{(R_1+R_2)}{sCL_1L_2}+D} \tag{2}$$

$$A = \frac{(R_1L_2+R_2L_1+R_3L_1+R_3L_2)}{L_1L_2} \tag{3}$$

$$D = \frac{(R_1+R_2)C+(L_1+L_2)}{CL_1L_2} \tag{4}$$

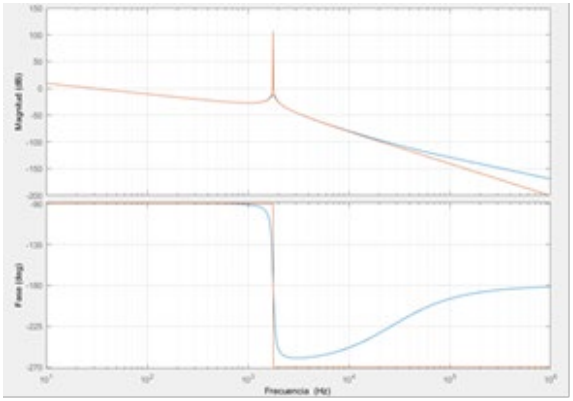

Fig. 2. Bode plot of the function $G_v(s)$ with $R_3 = 0\ \Omega$ (in red) and with attenuation $R_3 = 1\ \Omega$ (in blue).

It can be noticed that $G_v(s)$ has a resonance frequency which is given by:

$$\omega_r = \sqrt{\frac{(L_1+L_2)}{C \cdot L_1 \cdot L_2}} \quad (5)$$

For the calculation of (2), it has been imposed that the voltage at the output of the filter (connection point to the grid) $V_2 = 0$, as is usual in the literature [7]-[9].

This assumption, $V_2 = 0$, implies that the transfer function $G_v(s)$ aligns with the scenario where the short-circuit impedance is negligible, meaning it corresponds to the case of a high or ideal short-circuit power grid. To analyse the influence of considering the real network, the laboratory grid has been characterised, which is an extremely weak grid. The values obtained experimentally are shown in Table I.

Table I. - Parameters of the laboratory grid equivalent.

Parameter	Value	Description
R_{cc}	50.7 mΩ	Grid resistance
L_{cc}	1.14 mH	Grid inductance
L_{Tra}	1 mH	Grid connection transformer inductance

To obtain the transfer function without neglecting the short-circuit impedance Z_{cc} of the grid, the resulting equivalent circuit shown in Fig. 3 is considered, in which grid harmonics are neglected and the circuit at the fundamental frequency is not considered.

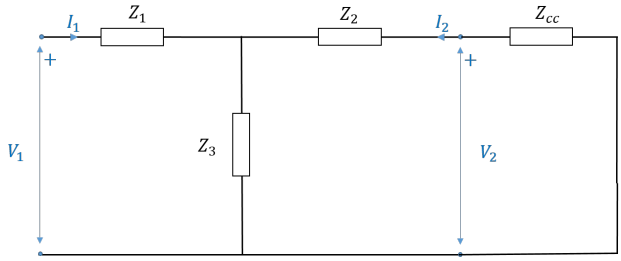

Fig. 3. Equivalent circuit of the filter considering grid effects.

From the analysis of the circuit in the complex frequency domain s, the following is obtained:

$$F_v(s) = \frac{-I_2}{V_1} = \left\{\frac{1}{Z_1} - \frac{V_2}{V_1} \cdot \left(\frac{Z_1+Z_3}{Z_1 \cdot Z_3}\right)\right\} \cdot \left\{\frac{Z_1 \cdot Z_3}{Z_1 \cdot Z_2 + Z_1 \cdot Z_3 + Z_2 \cdot Z_3}\right\} \quad (6)$$

3. Results

Using equations (2) and (6) yields nearly identical results (see Fig.2) when considering the ideal grid. However, when considering the real grid without damping resistance, the result varies slightly. Now, two resonance frequencies appear in the function $F_v(s)$ (at 1594 Hz and 1768 Hz), in addition to an anti-resonance frequency.

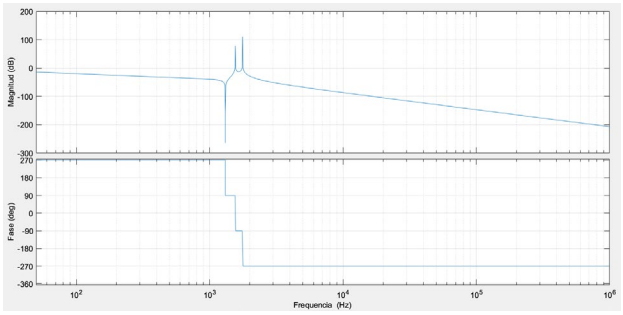

Fig. 4. Bode plot of the function $F_v(s)$.

As in the previous case, with the ideal grid, the resulting transfer function is unstable. Therefore, the conclusion in this case as well is the need to include a damping resistor to ensure system stability, although it reduces efficiency. An alternative that maintains efficiency is the application of a notch filter in the control, although this introduces a delay and, therefore, may contribute to worsening stability.

In the case of the 20 kW SiC inverter with LCL filter ($L_1 = 145\ \mu H, L_2 = 1\ mH, C = 20\ \mu F$) [10], the RC branch is analyzed, thus with passive damping that allows for maximum efficiency in harmonic reduction and loss minimization. From Nyquist analysis of the frequency response of $F_v(s)$, it is found that it is stable for values of $R_3 = 0.26\ \Omega$, but it becomes unstable when $R_3 = 0\ \Omega$.

The damping resistor R_3 value should be sufficient to prevent resonances that jeopardize the stability of the grid. However, the inclusion of resistor R_3 in series with the capacitor incurs associated losses (proportional to the square of the voltage applied to R_3), which at 50 Hz are negligible and increase as the frequency of the generated harmonic increases. These losses, according to the literature, are greater when R_3 is smaller, although increasing the damping resistance reduces the effectiveness of the LCL filter. Therefore, as already indicated, the value of resistor R_3 is established within an order of magnitude similar to that of the capacitor impedance in series at the resonance frequency ω_r [6],[7],[11], according to:

$$R_3 = \frac{1}{3 \cdot \omega_r \cdot C} \quad (7)$$

For a C=20 μF, a resonance frequency of f_r = 3162 Hz is obtained, with a damping resistor value of $R_3 = 0.839\ \Omega$.

In Table II, the results obtained by simulation considering the model of the inverter powered by a photovoltaic panel producing 16197 W and connected to the laboratory grid are shown. The control is the real one implemented in the prototype of the 20 kW SiC inverter, which is deployed from Simulink to the FPGA used. In the simulation, in addition to the losses due to the damping resistor, the values of THD in the output current I_2 and in the voltage V_2 at the connection point are also measured. The THD values have been measured considering, according to standard, up to the 40th harmonic (THD_{40}) and considering the entire spectrum up to the 5000th harmonic (THD_{∞}).

Table II. - Losses and harmonics in the 20 kW SiC inverter for different values of R_3 when $C = 20\ \mu F$.

R_3	Losses	$\text{THD}_{40}\ I_2$	$\text{THD}_{\infty}\ I_2$	$\text{THD}_{40}\ U_2$	$\text{THD}_{\infty}\ U_2$
17 Ω	230 W	3.42%	3.47%	1.77%	16.62%
8.5 Ω	170 W	1.81%	1.84%	1.09%	9.44%
2.5 Ω	70 W	1.21%	1.22%	0.85%	3.06%
0.8 Ω	37 W	1.08%	1.09%	0.78%	1.38%
0.5 Ω	27 W	1.08%	1.10%	0.81%	1.25%
0.26 Ω	20 W	0.92%	0.97%	0.71%	1.35%
0 Ω	Unstable	-	-	-	-

The results show losses that increase as R_3 increases, contrary to what is expected according to the literature. This is explained by the variation in harmonic content in the voltage applied to the RC branch. For low values of R_3, inductance L_1 achieves better filtering, resulting in lower voltage applied to R_3, while for high values, the harmonic component values in voltage increase.

The Table II clearly shows that the lower the value of R_3, the lower the THD in both current and voltage. Likewise, it is observed that even for values below 2.5 Ω, the THD values do not vary excessively.

It is remarkable to note how the system operates better below the values of R_3 determined by (7). It is worth highlighting that the system is not stable when operating without damping resistance, as expected. Based on these results, a value of $R_3 = 0.5\ \Omega$ is chosen for experimental measurements.

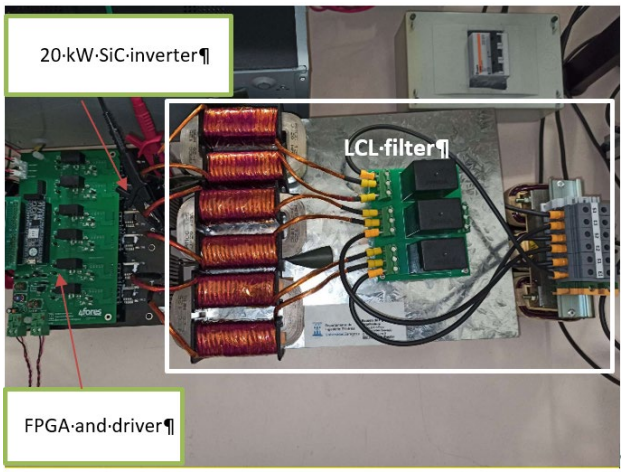

Fig. 5. 20 kW SiC inverter and the LCL filter prototype.

Table III shows the THD measured with the SiC inverter and a comparison with Si inverter (6.5 kW) for the switching frequencies considered.

Table III. - Si and SiC technologies comparison.

Technology	Switching Frequency	THD (%) Before Filter	THD (%) After Filter
Si	5 kHz	77%	4.5%
SiC	25 kHz	15%	0.32%

The LCL filter for the SiC inverter is able to reduce the THD down to 0.32% which significantly improves the result obtained with a Si inverter considering a similar filter. The LCL filter has been designed for a prototype, with a rated active power of 20 kW and a switching frequency of 25 kHz.

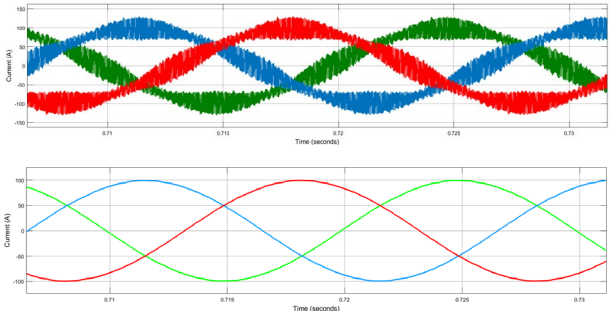

Fig. 6. Current waveforms of the inverter-side and the grid-side of the SiC inverter.

4. Conclusions

The analysis of an LCL filter for a 20 kW power inverter with a 25 kHz switching frequency has been conducted, obtaining its transfer function without neglecting the network effect. This paper also examines the optimal value of the damping resistor to minimize losses without compromising the stability of the device, as may occur with notch filtering.

The damping resistor values are much lower than those proposed in the literature, thus improving the efficiency of the device and reducing harmonic content. Finally, experimental harmonic content values are provided.

Acknowledgements

The authors would like to thank the technical support from the Research Group on Renewable Energy Integration (GENER) of the University of Zaragoza (accredited and funded by the Government of Aragon).

This research has received funding from the Spanish MCIN/AEI/10.13039/501100011033 under grant agreement No CPP2021-008848 and from the European Union NextGenerationEU/PRTR.

References

[1] X. Zhang, "Passive component weight reduction for three phase power converters", Doctoral thesis, Faculty of the Virginia Polytechnic Institute and State University Blacksburg, Virginia (2014), [Online], Available: https://vtechworks.lib.vt.edu/handle/10919/47788.

[2] Y. Liu, "Filter design of high power density converter with weight, size and thermal considerations", Doctoral thesis, Nanyang Technological University, Singapore (2018). [Online], Available: https://doi.org/10.32657/10356/74087.

[3] IEC 61000-2-2:2002, "Electromagnetic compatibility (EMC) - Part 2-2: Environment - Compatibility levels for low-frequency conducted disturbances and signalling in public low-voltage power supply systems", Edition 2.0, 2002.

[4] S. Takahashi, S. Ogasawara, M. Takemoto, K. Orikawa and M. Tamate, "Experimental Evaluation of the Relationship between Filter Inductor Impedances and Dimensional Resonances of MnZn Ferrites", 2019 IEEE 4th International Future Energy Electronics Conference (IFEEC), Singapore (2019), pp. 1-8, doi: 10.1109/IFEEC47410.2019.9015169.

[5] Y. Liu, K.Y. See, S. Yin, R. Simanjorang, C. F. Tong, A. Nawawi and J.-S. J. Lai, "LCL Filter Design of a 50-kW 60-kHz SiC Inverter with Size and Thermal Considerations for Aerospace Applications", IEEE Transactions on Industrial Electronics (2017). Vol. 64, No.10, pp. 8321-8333. doi: 10.1109/TIE.2017.2677338.

[6] R. Peña-Alzola, M. Liserre, F. Blaabjerg, R. Sebastián, J. Dannehl and F. W. Fuchs, "Analysis of the Passive Damping Losses in LCL-Filter-Based Grid Converters", IEEE Transactions on Power Electronics (2013), Vol. 28, No. 6, pp. 2642–2646. doi: 10.1109/TPEL.2012.2222931.

[7] A. Reznik, M. G. Simões, A. Al-Durra and S. M. Muyeen, "*LCL* Filter Design and Performance Analysis for Grid-Interconnected Systems", IEEE Transactions on Industry Applications (2014), Vol. 50, no. 2, pp. 1225-1232. doi: 10.1109/TIA.2013.2274612.

[8] Mohamed Azab, "Multi-objective design approach of passive filters for single-phase distributed energy grid integration systems using particle swarm optimization", Energy Reports (2020), Vol. 6, pp. 157-172, https://doi.org/10.1016/j.egyr.2019.12.015.

[9] P. Channegowda and V. John, "Filter Optimization for Grid Interactive Voltage Source Inverters", IEEE Transactions on Industrial Electronics (2010), Vol. 57, no. 12, pp. 4106-4114, Dec. 2010, doi: 10.1109/TIE.2010.2042421.

[10] S. Martín-Arroyo, J. A. Cebollero, M. García-Gracia and Á. Llamazares, "Stand-Alone Hybrid Power Plant Based on SiC Solar PV and Wind Inverters with Smart Spinning Reserve Management", Electronics (2021), Vol. 10, No. 796. https://doi.org/10.3390/electronics10070796.

[11] V. Blasko and V. Kaura, "A novel control to actively damp resonance in input LC filter of a three-phase voltage source converter", IEEE Transactions on Industry Applications (1997), Vol. 33, No. 2, pp. 542–550. doi: 10.1109/28.568021.